in silico Plants Vol. 3, No. 2, pp. 1–10
https://doi.org/10.1093/insilicoplants/diab025
Advance Access publication 14 August 2021
Original Research

in silico Plants

OXFORD

Row orientation affects the uniformity of light absorption, but hardly affects crop photosynthesis in hedgerow tomato crops

Maarten van der Meer[1,], Pieter H. B. de Visser[2], Ep Heuvelink[1] and Leo F. M. Marcelis[1,*,]

[1]Horticulture and Product Physiology, Wageningen University, Droevendaalsesteeg 1, 6708PB Wageningen, The Netherlands
[2]Business Unit Greenhouse Horticulture, Wageningen University, Droevendaalsesteeg 1, 6708PB Wageningen, The Netherlands
*Corresponding author's e-mail address: leo.marcelis@wur.nl

Handling Editor: Graeme Hammer

Citation: van der Meer M, de Visser PHB, Heuvelink E, Marcelis LFM. 2021. Row orientation affects the uniformity of light absorption, but hardly affects crop photosynthesis in hedgerow tomato crops. *In Silico Plants* **2021**: diab025; doi: 10.1093/insilicoplants/diab025

ABSTRACT

Light distribution within canopies is important for plant growth. We aimed to quantify the influence of row orientation on inter- and within-row variation of light absorption and photosynthesis in a hedgerow crop. An experiment with two row orientations of a tomato crop was conducted which was then used to calibrate a functional–structural plant model (FSPM). The FSPM was used to analyse light absorption and photosynthesis for each of the row facing directions in the double-row trellis system (e.g. north- and south-facing rows for the east–west row orientation). The measured leaf area decreased by 18 % and specific leaf area by 10 %, while fruit dry weight increased by 7 % for south-facing compared to north-facing rows, but total plant dry weight did not significantly differ. Model simulations showed a 7 % higher light absorption for the south-facing rows than north-facing rows, while net photosynthesis was surprisingly −4 % lower, due to local light saturation. When in the model leaf area was kept equal between the rows, light absorption for the south-facing rows was 19 % and net photosynthesis 8 % higher than for north-facing rows. We conclude that although south-facing rows would be expected to have a higher photosynthesis than north-facing rows, plants can adapt their morphology such that differences in light absorption and photosynthesis between north- and south-facing rows are minimal. Rows oriented north–south were more uniform in light absorption and photosynthesis than east–west rows, but the overall crop light absorption and photosynthesis were minimally affected (both 3 % lower compared to east–west orientation).

KEYWORDS: Functional–structural plant model; light absorption; photosynthesis; row orientation; spatial uniformity; tomato canopy.

1. INTRODUCTION

Plant positioning in rows causes inter- and intra-row shading, which affects the light distribution and pattern throughout the whole day (Trentacoste *et al.* 2016; Campos *et al.* 2017). Inter- and intra-row shading have been experimentally studied in relation to weed control (Borger *et al.* 2010; Johnson and Davis 2015; Borger *et al.* 2016) and hedgerow productivity and fruit quality (review by Trentacoste *et al.* 2015). For weed control, row orientation is manipulated such that the crop will cast shadow on the weeds, which can reduce weed growth due to lack of sunlight (Borger *et al.* 2010; Johnson and Davis 2015; Borger *et al.* 2016). For hedgerow productivity and product quality, a north–south row orientation is often favourable as reviewed by (Trentacoste *et al.* 2015). These authors argued that this is the result of a more equal distribution of light to the most important leaves and fruits between both east- and west-facing parts of the rows during a day in a north–south row orientation. A south-facing side can be light-saturated, while the north-facing side of a tree is still limited by light, resulting in unequal fruit set (Khemira *et al.* 1993), fruit abortion or

fruit rot (Lombard and Westwood 1977). Model simulations revealed that a certain canopy porosity could be required to support proper fruit growth in olives (Connor *et al.* 2009).

Process-based models (PBMs) have been used to simulate row orientation effects on light absorption and crop production of hedgerows. Studies using PBMs revealed that the effect of row orientation on light absorption and productivity depends on architecture, season and latitude (Mutsaers 1980; Gijzen and Goudriaan 1989). A north–south row orientation results in increased light absorption in summer at lower latitudes of 15–55° (Mutsaers 1980). The ratios between path width, row width and row height have major consequences for row orientation effects. Differences in light absorption and photosynthesis between row orientations diminish as the ratio between path width and row height decreases. When this ratio drops below 0.3 differences between row orientations become very small (Gijzen and Goudriaan 1989).

Functional–structural plant models (FSPMs) explore and integrate relationships between a plant's structure and processes that underlie its growth and development (Louarn and Song 2021). These models have been developed for several crops and for many purposes (Louarn and Song 2021) also for the study of plant architecture effects on light interception and distribution in a canopy (e.g. Buck-Sorlin *et al.* 2011; Cieslak *et al.* 2011; Wiechers *et al.* 2011; Chen *et al.* 2014). Sarlikioti *et al.* (2011) developed a 3D static FSPM for tomato to study the responses of light absorption and photosynthesis in relation to plant architecture at the leaf level for inter- and intra-canopy shading. Their preliminary study suggested that in both summer (June) and winter (December) at a latitude of 52° light absorption in a north–south row orientation is higher than in an east–west row orientation. Light distribution in canopies is important for crop photosynthesis as suggested by the modelling study of Sarlikioti *et al.* (2011) and as evidenced by the increased crop photosynthesis and growth of greenhouse grown tomato when the light is made more diffuse (Li *et al.* 2014). Considering the importance of a uniform light distribution within a canopy, the aim of this study is to quantify the influence of row orientation on the inter- and within-row variation of light absorption and photosynthesis in a hedgerow crop. Therefore, an experiment with two different row orientations of a tomato crop was conducted, which was then also used to adapt and calibrate a tomato FSPM. By doing so it was possible to (i) compare the growth and architecture of both rows in the north–south and east–west row orientations, (ii) explain the findings with the tomato FSPM by quantifying the light absorption and photosynthesis at leaf level for each of the rows and (iii) use the tomato FSPM to quantify light absorption and photosynthesis differences between rows at varying latitudes and seasons.

2. MATERIALS AND METHODS

2.1 Growth conditions

Tomato plants (*Solanum lycopersicum* cv. Capriccia) were grown in two adjacent glasshouse compartments at Wageningen University (52°N, 5.7°E). In one compartment the plant rows were oriented from north to south, and in the other from east to west. On 8 March 2016, 5 weeks after sowing, the plants were transplanted onto gutters on rockwool slabs. The plants were grown until 20 July 2016. The crop was managed according to grower practice. Nutrient solution (EC: 2.8 and pH: 5.5; **see Supporting Information—Table 1**) was provided daily in a frequency matching solar radiation. Side stems were removed weekly, and from 13 April onward the bottom three leaves were removed every week. From 25 April the plants reached the high wire at a height of 3.3 m, after which they were lowered weekly. The plants were grown in double rows, with distance of 50 cm between the single rows.

Distance between the mids of two adjacent double rows was 160 cm, resulting in a path of 62 cm (distance between outer leaves of each row). The distance between plants in a each single row was 50 cm. Stem density was 2.5 stems per m^2 until 7 April, when a secondary shoot was allowed to develop in the leaf axil directly below the fourth truss, thus raising the stem density to 5.0 stems per m^2. On 20 May a number of plants were removed for destructive harvests (and some additional plants) from each row to achieve the targeted 4.4 stems per m^2. Trusses were pruned to 6 fruits per truss. The CO_2 concentration was targeted at 600 ppm when the windows were closed and 400 ppm when the windows were open. Inside each compartment, a Hoogendoorn Box (Hoogendoorn, The Netherlands) was installed monitoring the climatic conditions at a 5-min interval. Averaged daily temperature, relative humidity and CO_2 (±standard deviation) over the whole growth period were 20.1 (±3.6) and 20.0 (±3.4) °C, 74.6 (±10.5) and 74.1 (±10.1) % relative humidity and 509 (±97) and 518 (±94) ppm CO_2 for each compartment with, respectively, north–south and east–west row orientation. The two glasshouse compartments were oriented −24° North–South. On the east, west and north side they were surrounded by other compartments, while there was a corridor on the south side. There was no artificial lighting present in surrounding compartments. Height of the greenhouse was 5 m and the rockwool slabs were 0.3 m above the floor. A picture of the plants in the greenhouse is shown in **Supporting Information—Fig. 1**).

2.2 Plant measurements

2.2.1 Architecture and dry weight Dry weight of ripe fruits was recorded of 12 plants of each of the north-, south-, east- and west-facing rows (in the middle of the compartments) during the whole experiment by weekly removal and weighing of trusses with fruits in stage 3 ('turning') up to stage 6 ('red') (Camelo and Gómez 2004). For each row facing side, three main stems were randomly selected from four centre rows for destructive measurements on 20–22 April, 17–20 May and 19–20 July. At each measurement day plant architecture was measured and dry weights of stem, leaves and fruits were determined for these three plants. On the measurements of 17–20 May and 19–20 July also three secondary stems were measured. Architectural measurements consisted of leaf area, as measured by a leaf area meter (LI-3100C, LI-COR, USA), leaf length, which was measured from the base of the petiole to the tip of the terminal leaflet using a ruler, and internode length. Plant material was dried in a ventilated oven at increasing temperature steps from 45 to 70 to 105°C, each for 24 h.

Additional measurements were performed for model development during the final harvest. One plant of each row facing side was measured to get an estimate of parameters that were necessary for building the model architecture, but were considered non-significantly different for both row orientations. These parameters were petiole angle, petiolule angle, leaflet angle and curvature, leaf area ratio between small

and big leaflets, rachis to petiolule length, the ratio between petiolule length to leaf area, leaflet length-to-width ratio and the rachis bend at the first and second big leaflet pairs, counted from the petiole to the tip of the leaf. These measurements were performed on leaves on ranks 1 to 3, 5 to 7, 10, 14, 18 and 22, counted from above. Rank 4, 8, 12, 16, 20 and 24 did not carry a leaf but truss of fruits. For the rank numbers of 10 and higher, the parameters for the measured leaves were assumed to hold for one rank below and above the measured rank.

2.2.2 Gas exchange The response of net photosynthesis rate (A; μmol m^{-2} s^{-1}) to light intensity and leaf internal CO_2 partial pressure (C_i) was determined on three different heights in the canopy: 50, 80 and 150 cm from the top, which refer to leaves 7, 10 and 16, respectively. Measurements dates for this were, respectively, 10–11, 16–17 and 25–26 June, with each height taking 2 days. At each height, gas exchange was measured with the LI-6400 photosynthesis system (LI-COR), equipped with the LI-6400 fluorescence cuvette (2 cm^2 leaf area) on two leaves for each row facing side. For each measured leaf, the leaf was enclosed in the cuvette at 1400 μmol m^{-2} s^{-1} photosynthetically active radiation (PAR) (90 % red, 10 % blue), 600 μbar CO_2 partial pressure, temperature of 28 ± 3 % fixed according to ambient temperature at start of measurements, relative humidity at 70 ± 10 % and a flow rate of 400 μmol m^{-2} s^{-1}. After A stabilized (≈15 min), CO_2 partial pressure was decreased in steps to 400, 300, 200, 100, 50 and 0 μbar. Then, CO_2 partial pressure was increased to 600 μbar, and after A stabilized (≈10 min) the CO_2 partial pressure was further increased to 800, 1200 and 1600 μbar. Then, CO_2 partial pressure was decreased to 700 μbar and light intensity was raised to 1800 μmol m^{-2} s^{-1}. After A stabilized (≈15 min), the light intensity was decreased in steps to 1450, 1100, 750, 450, 225, 100, and 0 μmol m^{-2} s^{-1}. At each CO_2 and light intensity step, the sample cell was calibrated against the reference cell, and A and C_i were recorded after this.

2.3 Model description

An adapted version of a static greenhouse tomato FSPM (de Visser *et al.* 2014) was used. The adaptation consisted of a modified leaf reconstruction by replacing each single parallelogram that represented a leaflet by 6–8 parallelograms that together represent the leaflet geometry more precisely [**see Supporting Information—Fig. 6**]; a larger number of parallelograms did not improve the simulated light absorption [**see Supporting Information—Table 3**]. This model was developed on the GroIMP platform (Kniemeyer 2008) and consists of an architectural, photosynthesis and light module.

2.3.1 Architectural module The architectural parameter values for leaf area, stem length and leaf length were taken from data at the phytomer level acquired from the final destructive measurement on 20 July (Table 2). Leaf area differed significantly between north- and south-facing rows and was implemented as such. All other variables were non-significantly different ($P < 0.05$) and were averaged within each row orientation; e.g. stem length for north- and south-facing rows was averaged together and the averaged value was taken for both north- and south-facing rows in the simulations. For additional required model parameters that were not in the scope of this study a limited number of replicate measurements were taken and averaged, namely petiole angle, first and second rachis bend [**see Supporting Information—Table 2**]. Leaf curvature was assumed 60° and the number of leaflets were considered 11 (three bigger pairs, two smaller pairs and one terminal leaflet; **see Supporting Information—Fig. 8**). The leaf area was then distributed across the 11 leaflets on each leaf according to an empirical allometric relationship. The area of the composite leaf was distributed over the five leaflet pairs and the terminal leaflet for each leaf in the same manner, using the following fractions (from proximal to distal leaflet pair): 0.1296, 0.0188, 0.1516, 0.0281, 0.0948 and the terminal leaflet with 0.1541. The length of the petiole was 35 % of the total leaf length, and at that point the first leaflet pair was attached [**see Supporting Information—Fig. 8**]. The actual leaf area depended on the observed relationship with leaf rank. No collision avoidance of leaves was computed, since leaves of neighbouring plants do in reality not show distinct avoidance mechanisms and extremely intertwine. Then, each plant was constructed in the simulation with a random phyllotaxis initiation [**see Supporting Information—Fig. 9**] oriented randomly after randomly deciding the first phyllotaxis angle. We assumed that the absence of collision avoidance in modelling leaf orientation was reasonable since leaves strongly intertwine when touching another at lower parts in the crop, and so leaflets may well be oriented rather randomly. The spaces between the leaflets of the leaf allow easy penetration of the leaf environment of the neighbouring plant. Moreover, during plant management operations (leaf cutting, fruit harvesting, shifting plant position in the row weekly) the leaves of neighbouring plants are often reshuffled and become slightly mixed in a random way. Above all, this mechanical process is appearing in both row treatments equally and will not affect treatment effects. Vermeiren *et al.* (2020) used a similar light model as we did and concluded that a simplification of the leaflet shape in a tomato crop can lead to small deviations in simulations of light absorption and gross photosynthesis. At the canopy level, this effect is mitigated somewhat by the canopy closure in dense canopies.

2.3.2 Photosynthesis module An adapted Farquhar–von Caemmerer–Berry model (FvCB model) was used to simulate photosynthesis Farquhar *et al.* 1980; Qian *et al.* 2012). All photosynthesis parameter values were kept the same as Qian *et al.* (2012), with exception of J_{max28} (μmol m^{-2} s^{-1}; maximum electron transport rate at 28°C) and V_{cmax28} (μmol m^{-2} s^{-1}; the maximum carboxylation capacity if Rubisco is fully activated at 28°C). Values for J_{max28} and V_{cmax28} were estimated from gas exchange measurements. Comparison of light response curves between leaves 7 and 10 showed such small differences in A_{max} (<4 %) that these were considered equal for leaves 7 and 10. J_{max28} and V_{cmax28} were assumed to decrease exponentially from the 10th leaf to the oldest leaf, as a result of age. This most basic assumption was taken since there was no support for any other relationship. Besides this, model simulations have shown that overestimation of photosynthesis when acclimation of photosynthetic parameters with height in the canopy is not considered is minimal when the only light source is the sun (van Ieperen and Trouwborst 2008). Values for J_{max28} and V_{cmax28} were estimated at 235.6 and 136.0, respectively, for the 10 youngest leaves, and exponentially decreased to 145.8 and 67.7, respectively, for

the oldest leaf ($R^2 > 0.99$) by use of least-squares regression on light response curve data. This was done using the evolutionary solver in Excel, version 2016. α and θ were assumed constant throughout the whole canopy. The ratio between C_i and C_a was assumed constant at 0.7, as suggested by (Sinclair *et al.* 1984) for C_3 species. This is valid if C_a values are larger than 300 ppm. In the experiment C_a varied between 350 and 550, resulting from CO_2 enrichment. **Supporting Information—Figure 6** shows the fit of modelled and measured data of the response of net photosynthesis rate to light intensity and leaf internal partial pressure.

2.3.3 Light module The light in the 3D scene was simulated in hourly time steps with a ray tracer, called Flux Light Model, provided by GroIMP. The Flux Light Model was described in detail by Henke and Buck-Sorlin (2017). This ray tracer was based on an inversed path tracer with a Monte Carlo pseudo-random number generator as in Veach (1998). So, this light model differed from the light model used by Sarlikioti *et al.* (2011) that was based on radiosity. However, we expect not much differences between the two models. If applied with our currently used ray numbers, the ray tracer casts enough rays to illuminate each object in the scene and will thus be comparable to the radiosity model that simulates all rays from light source to objects within a specified bounding box; for details on the models we refer to Chelle and Andrieu (1998), Sarlikioti *et al.* (2011) and Henke and Buck-Sorlin (2017). The number of rays were 750 million and recursion depth was 10; these numbers were chosen such that a further increase would not improve simulation results [**see Supporting Information—Table 3**]. For diffuse radiation, the assumption was made of an overcast sky, where light sources were located according to azimuth at every 7.5° and zenith at every 15°. The fraction diffuse light depended on the atmospheric transmission as estimated from hourly measured global radiation outside the greenhouse (Spitters *et al.* 1986). The remainder fraction of light was direct light, and modelled as a point source of directional light, arriving from the hourly solar position (model from Goudriaan and Van Laar 1994). The leaf reflectance and transmittance for 5 nm wavebands from 400 to 700 nm were measured with a Lambda 1050 spectrophotometer (Perkin-Elmer Inc.) coupled to a snap-in light integrating sphere. Stem optical properties were assumed to be similar to leaf properties, while fruits were assumed to absorb all light colours except for green (unripe fruits) and red (ripe fruits) wavelengths that were reflected for 100 %. A schematic representation of azimuth and solar angle in relation to row orientation is presented in **Supporting Information—Fig. 2**. A comparison of simulated light extinction in a canopy with measured data and a Lambert–Beer extinction can be found in **Supporting Information—Fig. 10**.

2.4 Model scenarios

2.4.1 Row orientation light absorption and net photosynthesis Model simulations were run to study light absorption and photosynthesis for the full-grown canopy (last 2 months of the experiment; 20 May to 20 July). Hourly climatic data on CO_2, temperature and radiation were used as input and the model was run with hourly time steps. The relation between fraction direct solar light and total radiation can be seen in **Supporting Information—Fig. 4**. Calculations were performed for the centre 12 plants in the centre two double rows. For row orientation comparison, four model simulations were performed: $EW_{N4.6,S3.8}$ (east–west row orientation, with a differing leaf area index of 4.6 for north-facing rows and 3.8 for south-facing rows according to measurements), $EW_{N3.8,S3.8}$ (east–west row orientation, with an equal leaf area index of 3.8 for both north- and south-facing rows), $EW_{N4.0,S4.0}$ (east–west row orientation, with an equal leaf area index of 4.0 for both north- and south-facing rows; leaf area index was equal to that of the plants in the north–south row orientation according to measurements) and $NS_{E4.0,W4.0}$ (north–south row orientation, with leaf area equal for east- and west-facing rows according to measurements). In order to determine the sensitivity of the model to important assumptions, three additional model simulations were performed for $EW_{N4.6,S3.8}$: $EW_{N4.6,S3.8,Pn}$ (equal photosynthetic parameters through the whole canopy), $EW_{N4.6,S3.8,Fl}$ (flat leaves) and $EW_{N4.6,S3.8,Rc}$ (random leaflet curvatures between 0 and 120°).

2.4.2 Inter-row shading at different latitudes and seasons For inter-row shading in an E-W row orientation, a simulation study was run for three latitudes (0°, 26°N and 52°N) for different seasons of the year (21 March, 21 June, 21 December) where north- and south-facing rows were compared in an E-W row orientation. In this simulation, CO_2 was fixed at 600 ppm, temperature at 23 °C and direct light at 77 %. The chosen days of the year (80, 171 and 356) represent the spring equinox (21 March) and the summer and winter solstices (21 June, 21 December). For these simulations the architecture of plants for north- and south-facing rows was the same with equal leaf area and a leaf area index (LAI) of 3.8. Distance between mid of the double rows was 160 cm and path width 62 cm (distance between outer leaves of two rows). In order to determine the sensitivity of the model to important assumptions, three additional model simulations were performed, where either the row distance was lowered to 130 cm, row distance was increased to 190 cm or where the photosynthetic parameters were equal through the whole canopy.

2.5 Statistical analysis of experimental data

Final harvest dry weight data of stem and leaves, as well as architectural data on stem length, leaf area, leaf length and specific leaf area were compared between rows within each row orientation in each compartment using an *F*-test (general linear model with main/secondary stem as covariate; $P = 0.05$; $n = 6$). Cumulative plant dry weight over the growth period was estimated from fruit mass of 12 plants (12 main + secondary stems) for north-, south-, east- and west-facing rows (including the weekly harvested fruits). As the recorded stem and leaf weight of three main and three secondary stems at final harvest were non-significantly different between rows within the row orientations (Table 1), the average stem and leaf weight for each row facing side was added to each of the 12 main and secondary stem fruit weights. Besides this, pruned leaf weight was estimated by averaging the leaf weight of the bottom 12–15 leaves at three consecutive harvests, comprising an average of 12 plants total per row facing side, and multiplying this with the total number of leaves harvested over time. Finally, effects of row facing side on cumulative plant dry weight and fruit dry weight per plant were tested within each row orientation using an *F*-test with row

Table 1. Measured values of dry weight of individual plant parts and cumulative plant dry weight (g DW per plant; mean ± SE) of the rows with different facing sides for plants grown in E-W and N-S oriented rows. Values marked in bold indicate significant differences between both row facing sides within the same row orientation.

		E-W orientation			N-S orientation		
Parameter	Stem	N_{facing}	S_{facing}	P-value	E_{facing}	W_{facing}	P-value
Stem	Main	45.7 ± 1.3	45.6 ± 3.1	0.476	43.5 ± 1.7	44.9 ± 3.1	0.369
	Secondary	35.3 ± 2	39.1 ± 3.2		35.0 ± 1.8	36.8 ± 0.6	
Leaf	Main	38.5 ± 1.9	35.7 ± 3.4	0.442	33.8 ± 0.2	35.6 ± 3.5	0.215
	Secondary	30.6 ± 2.2	29.2 ± 3		27.9 ± 3.4	32.2 ± 2.1	
$Leaf_{removed}$	Main	141.8	135.3	—	140.7	139.4	—
	Secondary	61.8	59		61.3	60.7	
Fruit	Main	195.6 ± 5.2	213.4 ± 5.0	**0.038**	211.4 ± 9.8	211.0 ± 4.6	0.726
	Secondary	84 ± 5.0	85.5 ± 2.4		86.6 ± 4.4	83.3 ± 3.1	
$Stem_{base}$	—	34 ± 1.1	33.8 ± 1.7	0.955	32.9 ± 1	34.7 ± 1.5	0.309
Total	—	667.2 ± 8.9	676.7 ± 7.8	0.268	673.1 ± 13.7	678.6 ± 5.8	0.804

Table 2. Measured values of plant architectural parameters leaf area, stem length, leaf length and specific leaf area at the end of the experiment (20 July) of the rows with different facing sides for plants grown in E-W and N-S oriented rows. Data did not include leaves removed during the experiment. Values shown are the averages (±SE) of the whole plant including main and secondary heads. Values marked in bold indicate significant differences between both facing sides within the same row orientation.

		E-W orientation			N-S orientation		
Parameter	Unit	N_{facing}	S_{facing}	P-value	E_{facing}	W_{facing}	P-value
Leaf area	cm^2	10 356 ± 564	8745 ± 470	**0.006**	8586 ± 533	9416 ± 477	0.150
Stem length	cm	443 ± 15	442 ± 19	0.926	423 ± 7	433 ± 18	0.224
Leaf length	cm	30.6 ± 0.5	29.3 ± 0.5	0.103	28.7 ± 0.6	29.1 ± 0.7	0.724
SLA	$cm^2\ g^{-1}$	301 ± 22	274 ± 18	0.221	280 ± 10	285 ± 21	0.844

as blocking factor (general linear model with three plants for each row facing side per double row as block; $P = 0.05$; $n = 4$). Normality and equal variances were assumed.

3. RESULTS

3.1 Experimental results

No significant differences were found for stem and leaf dry weight (g per plant) between the rows within the east–west as well as within the north–south row orientations (Table 1). Fruit dry weight (g per plant) was significantly higher (7 %) for the south-facing rows compared to the north-facing rows in the east–west row orientation. Between the east- and west-facing rows in the north–south row orientation there was no significant difference in fruit dry weight. No significant differences were found for cumulative plant dry weight between the rows within the east–west as well as within the north–south row orientations (Table 1).

Leaf area was 18 % higher for north-facing rows than south-facing rows in the east–west row orientation (Table 2). Specific leaf area (SLA) seemed to be 10 % higher for the north-facing compared to south-facing rows, though this difference was not statistically significant. Leaf area was non-significantly different between east- and west-facing rows in the north–south row orientation. No significant differences were found in stem length and leaf length between the rows within the east–west as well as within the north–south row orientations (Table 2).

3.2 Model simulations

3.2.1 Within-row orientation differences in light absorption and net photosynthesis Model simulations for the full-grown crop (20 May to 20 July) showed a clear relationship between global incoming PAR (μmol $m^{-2}\ s^{-1}$) and ΔPAR absorbed (μmol $m^{-2}\ s^{-1}$) and Δnet photosynthesis (μmol $m^{-2}\ s^{-1}$) for the east–west row orientations (Fig. 1, Δ denotes differences between the facing sides of rows; in this case between south- and north-facing rows). On days with low global incoming radiation, which are cloudy days with a larger fraction diffuse radiation, the north-facing row had a higher light absorption and net photosynthesis compared to the south-facing row. For $NS_{E4.0,W4.0}$ (both east- and west-facing row having LAI of 4) very minimal differences were found between east- and west-facing rows, only 1 % for PAR absorption and 0 % for net photosynthesis (Fig. 1). For $EW_{N4.6,S3.8}$ (north-facing row higher LAI than south-facing row) the differences were clear. Over the whole period, south-facing rows absorbed 7 % more light, but this still resulted in a lower net photosynthesis of −4 %. With leaf area equal for north- and south-facing rows

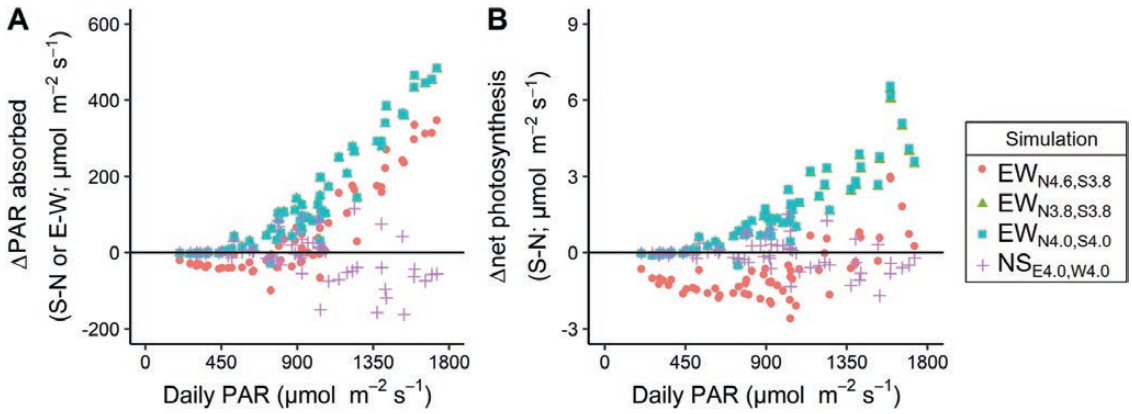

Figure 1. Simulated absolute differences in (A) PAR absorbed (μmol m^{-2} s^{-1}) and (B) net photosynthesis rate (μmol m^{-2} s^{-1}) between the two sides of a row versus incoming PAR (μmol m^{-2} s^{-1}); hence, difference between south- and north-facing rows in an E-W row orientation and between east- and west-facing rows in a N-S row orientation. '$EW_{N4.6,S3.8}$' denotes the model simulation where north-facing rows had a higher leaf area index than south-facing rows (leaf area index 4.6 versus 3.8 m^2 m^{-2}), whereas '$EW_{N3.8,S3.8}$' is the model simulation where north-facing rows and south-facing rows have equal leaf area index (3.8 m^2 m^{-2}). In '$NS_{E4.0,W4.0}$' both east- and west-facing rows have equal leaf area index (3.8 m^2 m^{-2}). Each data point refers to an entire plant and represents the value of 1 day (from sun rise to sun set) between 20 May and 20 July.

(simulation $EW_{N3.8,S3.8}$) the difference in light absorption of the south-facing rows compared to north-facing rows increased to 19 %, while net photosynthesis was 8 % higher. The model sensitivity analysis for $EW_{N4.6,S3.8}$ showed that the assumption of photosynthetic parameters had a slight 2 % change in daily net photosynthesis, while changing the leaf curvature to completely flat leaves increased daily PAR differences by 1 % [**see Supporting Information—Fig. 7**]. Model results were only minimally influenced by these parameters. In N-S rows the cumulative difference in PAR absorption and photosynthesis between the east- and west-faced row was less than 1 %. A comparison between $EW_{N4.0,S4.0}$ and $NS_{E4.0,W4.0}$ showed that $EW_{N4.0,S4.0}$ had a 3 % higher daily light absorption and net photosynthesis.

3.2.2 Inter-row shading in an east–west row orientation Biggest relative differences between south- and north-facing rows in PAR absorbed and net photosynthesis were found when the maximum solar angle during solar noon was about 60° (Fig. 2). On Day 80 biggest daily differences in PAR absorption between south- and north-facing row were found at latitude 26, while at Day 171 and 356 biggest differences were found at latitude 0. In these cases, the biggest differences were always found in the middle of the canopy [**see Supporting Information—Fig. 5**]. This was always paired with light-saturated conditions; hence, the relative differences in daily net photosynthesis rate are close to half that of differences in daily absorbed PAR. An example of this was for Day 356, where daily PAR differences were +55 % and photosynthesis differences only +28 % for latitude 0. For latitude 26 this was +25 % and +13 %. The fact that the biggest differences were found for the middle leaf layer indicates that most shading is taking place on the middle layer of the canopy.

Reducing the row distance from 1.6 to 1.3 m, thereby reducing path distance to 0.32 m, resulted in a lower maximum difference between north- and south-facing rows of 33 % instead of 61 % for latitude 26 on Day 80 [**see Supporting Information—Table 4**]. Differences in net photosynthesis were decreased by 10 % (from 32 to 22 %). Increasing the row distance from 1.6 to 1.9 m, thereby increasing path width to 0.92 m, resulted in a maximum difference in daily absorbed PAR between north- and south-facing rows of 73 % instead of 55 % for latitude 0 on Day 356. This resulted in an only small increase in differences of daily net photosynthesis of north- versus south-facing row from 28 to 32 %. Hence, modifying the row distance had clear effects on daily light interception, although effects were limited for daily net photosynthesis since most additional light captured was during light-saturated conditions. Removal of leaf photosynthetic aging in the model increased daily net photosynthesis differences between north- and south-facing rows by a maximum of 6 % for latitude 26 on Day 80.

4. DISCUSSION

4.1 Leaf area adaptation increased within-row net photosynthesis uniformity

Although the total plant mass was similar for north- and south-facing rows, south-facing rows produced substantially more fruit mass. Hence, dry matter partitioning differed between north- and south-facing plants. This could be due to a higher fruit temperature in the south-facing rows, when fruits were hanging below the leaves, at the stage in which they are more prone to heat maturation (Adams *et al.* 2001). Temperatures of tomato trusses on the outside of the canopy have been shown to be 1.9 °C higher than air temperature and 0.9 °C warmer than trusses in middle of the rows (Adams and Valdeés 2002). With south-facing rows receiving more light the higher temperatures could have resulted in faster fruit development (Qian *et al.* 2015) and potentially a higher partitioning towards the fruits (Adams *et al.* 2001).

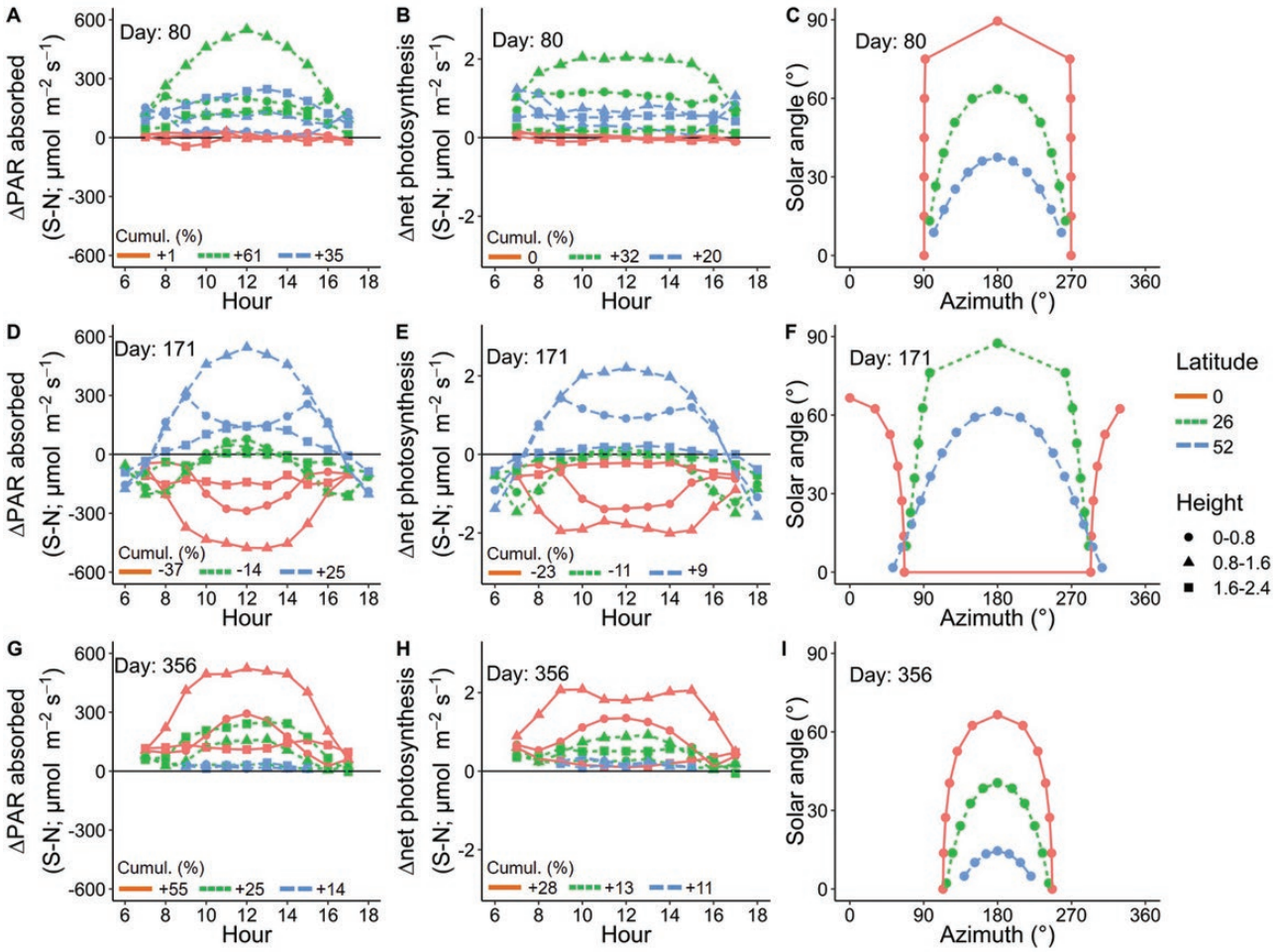

Figure 2. Hourly simulated PAR absorbed (A, D, G) and net photosynthesis (B, E, H), presented as differences (µmol m^{-2} leaf area s^{-1}) between south- and north-facing rows of east–west oriented rows for three different leaf layers from bottom to top of canopy (80 cm height interval each) at different latitudes (0, 26 and 52° Northern hemisphere) on days that represent the spring equinox (Day 80) and the summer and winter solstices (Day 171 and 356). Solar angle and azimuth are shown in C, F and I. Leaf area index of each canopy height (from bottom to top) was 1.43, 1.42 and 0.93 m^2 and was equal for the north- and south-facing rows. The numbers just above the *x*-axis represent cumulative differences over the whole day between the south- and north-facing rows. For schematic representation of azimuth and solar angle, we refer to Supporting Information—Fig. 2.

The increase in fruit dry weight was observed to have been compensated by a decrease in light absorption by a reduction in leaf area (Table 2). Surprisingly, north-facing plants adapted and had a larger total leaf area. This larger total leaf area partly compensated the lower light absorption per unit leaf area. An increase in leaf area is observed under shade avoidance symptoms (Kalaitzoglou *et al.* 2019). Another symptom, a decrease in leaf thickness (where more leaf area per gram of dry weight is required) (Holmes and Smith 1975; Smith and Whitelam 1997), was observed but found non-significant. Other typical shade avoidance responses were not found such as increased elongation of stems (Ballaré *et al.* 1991; Smith and Whitelam 1997; Cole *et al.* 2011), nor a change in leaf mass.

Model simulations with increased leaf area for plants in the north rows ($EW_{N4.6,S3.8}$) demonstrate that the increase in leaf area enhanced within-row uniformity in light absorption and net photosynthesis (Fig. 1). At the end of the period of 2 months, total simulated light absorption was 7 % higher for south-facing rows, while net photosynthesis rate was −4 %. To understand the difference in these relative effects on light absorption and net photosynthesis, we have to consider that during the period of the model simulations the climate consisted of days with varying light conditions. On completely cloudy days the north-facing rows had higher light absorption and higher net photosynthesis rate. On sunny days the south-facing rows absorbed more light than north-facing rows. However, during hours close to solar noon when intensity is high the effects of extra light on photosynthesis are relatively small (Fig. 2). This can also be seen in a frequency plot covering simulations of the whole 2 months [**see Supporting Information—Fig. 3**]. The assumptions of leaf curvature and photosynthetic aging

throughout the canopy had minimal influence on model result findings [**see Supporting Information—Fig. 7**]. Model simulations where leaf area was equal between north- and south-facing rows ($EW_{N3.8,S3.8}$) show that this would have resulted in a major difference between the two rows in light absorption and net photosynthesis of 19 and 8 %, respectively.

4.2 Light absorption and net photosynthesis similar between row orientations

In the current modelling study a minimal difference in light absorption and net photosynthesis was found for the period of 20 May to 20 July between both row orientations, with 3 % higher light absorption and net photosynthesis for the E-W row orientation ($EW_{N4.0,S4.0}$) compared to the N-S row orientation ($NS_{E4.0,W4.0}$). This is also in accordance with model simulations of Gijzen and Goudriaan (1989), who mentioned that row orientation is less influential at higher latitudes when the path width and row height ratio was in the range of ≤30 %. In this study, the path width was 62 cm and row height was 2.3 m, resulting in a ratio of 27 % between both. Similarly, the work of Maddonni *et al.* (2001) on plant spatial distribution in maize suggested that the plasticity of maize canopy results in similar daily light interception values in different inter-row distances. Furthermore, no differences were found within the N-S row orientation, in accordance with previous literature (Trentacoste *et al.* 2015).

4.3 Inter-row shading in an east–west row orientation

The model exploration showed that inter-row shading of south-facing on north-facing rows is highly season- and latitude-dependent, following similar patterns to that found in hedgerows by Trentacoste *et al.* (2016). The differences of 33 % between daily differences in light absorption and daily differences in net photosynthesis on Day 356 show that light saturation plays a large role in row orientations where inter-row shading occurs around solar noon. At higher angles the differences are largest when the azimuth is not following the equator. Similar to Trentacoste *et al.* (2016) we found that the biggest differences between north- and south-facing rows are found in the middle layer of the canopy, followed by the top and then the bottom of the canopy (Fig. 2). Different strategies could be explored to increase the uniformity in tomato production within the double rows. The sensitivity analysis showed that either reducing or increasing row distance by 30 cm had a quite large effect on light interception differences up to 28 %, although differences in photosynthesis did not exceed 11 % and thus remained similar. To reduce within-row differences between facing sides it could be worthwhile to prune leaves around the middle leaf layer of the south- or north-facing rows, as it has been shown that most light is absorbed by the middle leaf layer. This light could then penetrate to the next rows.

5. CONCLUSIONS

Despite the higher uniformity when rows were oriented north–south, the overall crop light absorption and photosynthesis were slightly higher for an east–west orientation (both 3 % higher). Due to plant adaptation, row orientation had a minimal influence on light absorption and net photosynthesis at 52°N, where east–west has a slightly higher light absorption and net photosynthesis. In an east–west row orientation, an increased leaf area for the north-facing rows compared to the south-facing rows enhanced the uniformity in light absorption and net photosynthesis. Here, despite inter-row shading and higher light absorption for the south-facing rows, dry weight production was unaffected due to light saturating conditions. Model explorations reveal that almost all competition for light occurs in the middle layer of the canopy, and that this is strongly dependent on season with differences in solar angle and azimuth. Model simulations for the spring equinox and the summer and winter solstices reveal that between north- and south-facing rows the differences in daily light absorption range from −37 % up to +61 %, whereas for daily net photosynthesis this range is between −23 % up to +32 %. Reducing the row distance or pruning leaves are clear strategies that minimize within double row differences in productivity.

SUPPORTING INFORMATION

The following additional information is available in the online version of this article—

Table S1. Composition of the nutrient solution used in the experiment. Solution EC: 2.8 and pH: 5.5.

Table S2. Architectural parameter values considered non-significantly different of petiole angle, rachis first bend and rachis second bend for different phytomer ranks.

Table S3. Percentual difference of modelled crop net photosynthesis and absorption of PPFD between model runs using default or other values of input parameters such as number of parallelograms per leaflet (6 to 14, with 8 as default), ray number (50 million to 1 billion, with 750 million as default) and recursion depth (1–15, where 10 is default). Simulations were done for one light condition on day 171 with diffuse sunlight and a plant density of 4.4 m^{-2}. For the default settings simulated daily averaged photosynthesis and crop light absorption were 36.16 μmol CO_2 m^{-2} s^{-1} and 1591.85 μmol PPFD m^{-2} s^{-1}.

Table S4. Daily differences in PAR absorption and net photosynthesis (%) between south- and north-facing rows in an E–W row orientation at different latitudes (0, 26 and 52° Northern hemisphere) on days that represent the spring equinox (day 80) and the summer and winter solstices (day 171 and 356). Leaf area index of the canopy was 3.8. Path and row width were 62 cm and 160 cm, respectively. Distance between both rows in a double row was 0.5 m.

Figure S1. Pictures taken during the experiment at 1 (A), 6 (B), 10 (C), and 14 weeks after transplanting (D, E).

Figure S2. Schematic representation of azimuth and solar angle, in relation to plants in a row with south-north orientation.

Figure S3. Frequency distribution of simulated PPFD absorbed by each individual leaflet during the whole two month period for north- and south-facing rows.

Figure S4. Simulated averaged daily direct light (%) versus daily incoming PAR (μmol m^{-2} s^{-1}) for the final two months of the experiment (20 May to 20 July).

Figure S5. Hourly simulated PAR absorbed (A, D, G) and net photosynthesis (B, E, H) (μmol m^{-2} leaf area s^{-1}) for south-facing rows in

east-west oriented rows for three different leaf layers (80 cm each) at different latitudes (0, 26 and 52° Northern hemisphere) on days that represent the spring equinox (day 80) and the summer and winter solstices (day 171 and 356). Leaf area index of each canopy height (from bottom to top) was 1.43, 1.42 and 0.93 m^2.

Figure S6. Measured (symbols) and modelled (lines) relation between net photosynthesis rate and (left) leaf internal partial pressure of CO_2 and (right) incident light intensity, at the middle-top (triangles; dotted line; 50–80 cm from the top) and bottom (crosses; dashed line; 150 cm from the top) of the canopy.

Figure S7. Sensitivity analysis EW1. Pn stands for equal photosynthetic parameter values throughout the entire canopy (no aging), Fl stands for flat leaves (0 degrees curvature in leaflets), Rc stands for random curvature (between 0 and 120 degrees), normally curvature of leaves is 60 degrees.

Figure S8. Simulated representation of a single leaf of a plant showing the number of leaflets and curvature. The place of the first and second bend of the rachis are depicted by respectively a red and a blue arrow.

Figure S9. Simulated representation of a single plant, based on average model parameters, showing the architecture of a plant. Parameters were based on architectural measurements in the experiment as described in section 2.2.

Figure S10. Comparison of simulated light extinction in the canopy compared with measurements and Lambert–Beer extinction (k = 0.75).

ACKNOWLEDGEMENTS

I would like to express my gratefulness to several people during the execution of this experiment. Andre Maassen, Geurt Versteeg, Maarten Peters, Sean Geurts, Erik Schuiling, Ferdinand Diesman for taking care of plant growth, maintenance and technical assistance. And to Nur Fauzana Mohd Kasim and Csongor Szanto for extensive help during the experiment.

SOURCES OF FUNDING

The project was funded by the Wellensiek Fund.

CONFLICT OF INTEREST

None declared.

CONTRIBUTIONS BY THE AUTHORS

M.v.d.M., P.H.B.d.V., E.H. and L.F.M.M. devised the project and the main conceptual ideas. M.v.d.M., P.H.B.d.V., E.H. and L.F.M.M. designed the experiment. M.v.d.M. executed the experiment and processed the experimental data. All authors were involved in data analysis. M.v.d.M. drafted the manuscript and designed the figures. All authors discussed the results and commented on the manuscript. L.F.M.M. initiated the project and acquired the funding.

LITERATURE CITED

Adams SR, Cockshull KE, Cave CRJ. 2001. Effect of temperature on the growth and development of tomato fruits. *Annals of Botany* **88**:869–877.

Adams SR, Valdeés VM. 2002. The effect of periods of high temperature and manipulating fruit load on the pattern of tomato yields. *The Journal of Horticultural Science and Biotechnology* **77**:461–466.

Ballaré CL, Scopel AL, Sánchez RA. 1991. Photocontrol of stem elongation in plant neighbourhoods: effects of photon fluence rate under natural conditions of radiation. *Plant, Cell & Environment* **14**:57–65.

Borger C, Hashem A, Pathan S. 2010. Manipulating crop row orientation to suppress weeds and increase crop yield. *Weed Science* **58**:174–178.

Borger CPD, Hashem A, Powles SB. 2016. Manipulating crop row orientation and crop density to suppress *Lolium rigidum*. *Weed Research* **56**:22–30.

Buck-Sorlin G, de Visser PH, Henke M, Sarlikioti V, van der Heijden GW, Marcelis LF, Vos J. 2011. Towards a functional-structural plant model of cut-rose: simulation of light environment, light absorption, photosynthesis and interference with the plant structure. *Annals of Botany* **108**:1121–1134.

Camelo AFL, Gómez PA. 2004. Comparison of color indexes for tomato ripening. *Horticultura Brasileira* **22**:534–537.

Campos I, Neale CMU, Calera A. 2017. Is row orientation a determinant factor for radiation interception in row vineyards?. *Australian Journal of Grape and Wine Research* **23**:77–86.

Chelle M, Andrieu B. 1998. The nested radiosity model for the distribution of light within plant canopies. *Ecological Modelling* **111**:75–91.

Chen TW, Henke M, de Visser PHB, Buck-Sorlin G, Wiechers D, Kahlen K, Stutzel H. 2014. What is the most prominent factor limiting photosynthesis in different layers of a greenhouse cucumber canopy? *Annals of Botany* **114**:677–688.

Cieslak M, Seleznyova AN, Hanan J. 2011. A functional-structural kiwifruit vine model integrating architecture, carbon dynamics and effects of the environment. *Annals of Botany* **107**:747–764.

Cole B, Kay SA, Chory J. 2011. Automated analysis of hypocotyl growth dynamics during shade avoidance in *Arabidopsis*. *The Plant Journal* **65**:991–1000.

Connor D, Centeno A, Gomez-del-Campo M. 2009. Yield determination in olive hedgerow orchards. II. Analysis of radiation and fruiting profiles. *Crop and Pasture Science* **60**:443–452.

de Visser PH, Buck-Sorlin GH, van der Heijden GW. 2014. Optimizing illumination in the greenhouse using a 3D model of tomato and a ray tracer. *Frontiers in Plant Science* **5**:48.

Farquhar GD, von Caemmerer S, Berry JA. 1980. A biochemical model of photosynthetic CO_2 assimilation in leaves of C_3 species. *Planta* **149**:78–90.

Gijzen H, Goudriaan J. 1989. A flexible and explanatory model of light distribution and photosynthesis in row crops. *Agricultural and Forest Meteorology* **48**:1–20.

Goudriaan J, Van Laar HH. 1994. *Modelling potential crop growth processes. Textbook with exercises*. Dordrecht: Springer-Science+Business Media.

Henke M, Buck-Sorlin, GH. 2017. Using a full spectral raytracer for calculating light microclimate in functional-structural plant modelling. *Computing and Informatics* **36**:1492–1522. doi:10.4149/cai2017 6 1492.

Holmes M, Smith H. 1975. The function of phytochrome in the natural environment. *Nature* **254**:512–514.

van Ieperen W, Trouwborst G. 2008. The application of LEDs as assimilation light source in greenhouse horticulture: a simulation study. *Acta Horticulturae* **801**:1407–1414.

Johnson WC, Davis JW. 2015. Perpendicular cultivation for improved in-row weed control in organic peanut production. *Weed Technology* **29**:128–134.

Kalaitzoglou P, van Ieperen W, Harbinson J, van der Meer M, Martinakos S, Weerheim K, Nicole CCS, Marcelis LFM. 2019. Effects of continuous or end-of-day far-red light on tomato plant growth, morphology, light absorption, and fruit production. *Frontiers in Plant Science* **10**:322.

Khemira H, Lombard P, Sugar D, Azarenko AN. 1993. Hedgerow orientation affects canopy exposure, flowering, and fruiting of 'Anjou' pear trees. *HortScience* **28**:984–987.

Kniemeyer O. 2008. *Design and implementation of a graph grammar based language for functional–structural plant modelling. PhD Thesis*, BTU, Cottbus.

Li T, Heuvelink E, Dueck TA, Janse J, Gort G, Marcelis LF. 2014. Enhancement of crop photosynthesis by diffuse light: quantifying the contributing factors. *Annals of Botany* **114**:145–156.

Lombard PB, Westwood MN. 1977. Effect of hedgerow orientation on pear fruiting. *HortScience* **69**:175–182.

Louarn G. Song Y. 2021. Two decades of functional-structural plant modelling: now addressing fundamental questions in systems biology and predictive ecology. *Annals of Botany* **14**:501–509.

Maddonnia GA, helleb MC, Drouetb J-L, Andrieu B. 2001. Light interception of contrasting azimuth canopies under square and rectangular plant spatial distributions: simulations and crop measurements. *Field Crops Research* **70**:1–13.

Mutsaers HJW. 1980. The effect of row orientation, date and latitude on light absorption by row crops. *The Journal of Agricultural Science* **95**:381–386.

Qian T, Dieleman JA, Elings A, de Gelder A, Marcelis LFM. 2015. Response of tomato crop growth and development to a vertical temperature gradient in a semi-closed greenhouse. *The Journal of Horticultural Science and Biotechnology* **90**:578–584.

Qian T, Elings A, Dieleman JA, Gort G, Marcelis LFM. 2012. Estimation of photosynthesis parameters for a modified Farquhar–von Caemmerer–Berry model using simultaneous estimation method and nonlinear mixed effects model. *Environmental and Experimental Botany* **82**:66–73.

Sarlikioti V, de Visser PH, Marcelis LF. 2011. Exploring the spatial distribution of light interception and photosynthesis of canopies by means of a functional-structural plant model. *Annals of Botany* **107**:875–883.

Sinclair TR, Tanner CB, Bennett JM. 1984. Water-use efficiency in crop production. *BioScience* **34**:36–40.

Smith H, Whitelam GC. 1997. The shade avoidance syndrome: multiple responses mediated by multiple phytochromes. *Plant, Cell & Environment* **20**:840–844.

Spitters CJT, Toussaint HAJM, Goudriaan J. 1986. Separating the diffuse and direct component of global radiation and its implications for modeling canopy photosynthesis: part I. Components of incoming radiation. *Agricultural and Forest Meteorology* **38**:217–229.

Trentacoste ER, Connor DJ, Gómez-del-Campo M. 2015. Row orientation: applications to productivity and design of hedgerows in horticultural and olive orchards. *Scientia Horticulturae* **187**:15–29.

Trentacoste ER, Gómez-del-Campo M, Rapoport HF. 2016. Olive fruit growth, tissue development and composition as affected by irradiance received in different hedgerow positions and orientations. *Scientia Horticulturae* **198**:284–293.

Veach E. 1998. *Robust Monte Carlo methods for light transport simulation. PhD Thesis*, Stanford University, California. http://graphics.stanford.edu/papers/veach_thesis/thesis-bw.pdf.

Vermeiren J, Villers SLY, Wittemans L, Vanlommel W, van Roy J, Marien H, Coussement JR, Steppe K. 2020. Quantifying the importance of a realistic tomato (*Solanum lycopersicum*) leaflet shape for 3-D light modelling. *Annals of Botany* **126**:661–670.

Wiechers D, Kahlen K, Stützel H. 2011. Evaluation of a radiosity based light model for greenhouse cucumber canopies. *Agricultural and Forest Meteorology* **151**:906–915.